

## Efficient analysis of SSI problems using infinite elements and wavelet theory

Mohamad Hossein Bagheripour, Reza Rahgozar\* and Mohsen Malekinejad

*Department of Civil Engineering, University of Kerman, Kerman, Iran*

*(Received July 18, 2010, Accepted October 20, 2010)*

**Abstract.** In this paper, Soil-Structure Interaction (SSI) effect is investigated using a new and integrated approach. Faster solution of time dependant differential equation of motion is achieved using numerical representation of wavelet theory while dynamic Infinite Elements (IFE) concept is utilized to effectively model the unbounded soil domain. Combination of the wavelet theory with IFE concept lead to a robust, efficient and integrated technique for the solution of complex problems. A direct method for soil-structure interaction analysis in a two dimensional medium is also presented in time domain using the frequency dependent transformation matrix. This matrix which represents the far field region is constructed by assembling stiffness matrices of the frequency dependant infinite elements. It maps the problem into the time domain where the equations of motion are to be solved. Accuracy of results obtained in this study is compared to those obtained by other SSI analysis techniques. It is shown that the solution procedure discussed in this paper is reliable, efficient and less time consuming as compared to other existing concepts and procedures.

**Keywords:** soil structure interaction; infinite elements; wavelet theory; fourier transformation; numerical analysis.

---

### 1. Introduction

Most dynamic and earthquake analyses of structures are performed neglecting the impact of the soil and the foundation on structural response. However, the effect of Soil-Structure Interaction (SSI) may be significant especially for stiff structures resting on soft soil deposits (Wolf 1985). Masia *et al.* (2004) discussed that soil-structure interaction is not limited to seismic analysis or design of special buildings such as reactor or framed building resting on mat foundations. The effects of SSI may also alter the dynamic characteristics of the structural response as well as that of the free field motion. Hence, a new combined dynamical system which includes the soil domain as well as the structure is developed while taking the SSI effects into account. As mentioned by Kramer (1996), seismic waves may travel through tens of kilometers of rocks and often less than 100 m of soil to reach the surface. Despite this, soil layers play a significant role in determining the characteristics of surface ground motion; since, as may be visualized from Fig. 1(a), these waves are often refracted and amplified. A complete review on the history of SSI was recently provided by

---

\*Corresponding author, Associate Professor, E-mail: [rahgozar@mail.uk.ac.ir](mailto:rahgozar@mail.uk.ac.ir)



This issue can be overcome by introducing infinite elements along the soil boundaries and is considered in this study. Bettles (1977) was apparently the first to introduce the formulation of infinite element in static analyses. For dynamic problems, Chow and Smith (1981), Zhao and Valliappan (1992) and Zhao and Zhang (1989) introduced and applied the dynamic infinite elements in various geomechanical problems. A comprehensive review on the types and formulations for both the static and dynamic infinite elements is found in Bagheripour and Marandi (2003). Kim and Yun (2000) have applied infinite elements to the SSI vibration analysis of a block foundation.

Main advantages of infinite elements are savings in modeling and computation times, reduction in cost without sacrificing the accuracy of computed solution. Furthermore, infinite elements have all the advantages of the conventional finite elements *i.e.* features such as a banded coefficient matrix and numerical integration procedures are retained.

In this paper, a new approach is adopted for the investigation of SSI effect on seismic response of structures resting on soil. Wavelet theory is used as a special tool for faster solving of time dependant differential equation of motion while dynamic Infinite Elements (IFE) are used to effectively model the unbounded soil domain. The use of wavelet theory associated with IFE provides an integrated, fast, efficient tool for solving complex SSI problems. In the followings, a brief discussion is given on the fundamental equations of motion in soil region based on wave propagation theory in visco-elastic medium is presented first; followed by discussion on infinite element formulation used in this study. Next, a concise description of the wavelets theory is given. Structural response spectrum that considers SSI effects is obtained using wavelet theory associated with the infinite elements (IFE). Comparing the results that include SSI effect with those that exclude the effect along with comparison to other SSI methods are used to validate the proposed scheme.

## 2. Equation of motion for SSI analysis

As mentioned earlier, in a direct SSI approach the entire soil-foundation-structure system is modeled and analyzed in a single stage. Input motions are specified along the base and on one side of the model. The response is computed using equations of motion in time domain *i.e.*

$$[M]\{\ddot{u}\} + [K^*]\{u\} = -[M]\{\ddot{u}_g(t)\} \quad (1)$$

where  $[M]$  and  $[K^*]$  are the mass and dynamic stiffness matrices respectively.  $u_g(t)$  is the specified ground motion at time  $t$  while its second derivative  $\ddot{u}_g(t)$  is the ground acceleration recorded during an earthquake. In fact,  $u_g(t)$  in the proposed framework may be assumed to be equal to free field motion (*i.e.*  $u_g(t) \cong u_{ff}(t)$ ). Equations of motion can be expressed in an alternative form by introducing the interaction force vector linking the near and far field soil regions and decomposition of mass and stiffness matrices. They can be demonstrated in both frequency and time domains by Eqs. (2) and (3) respectively (Kim and Yun 2000)

$$\begin{bmatrix} S_{ss}(\omega) & S_{sb}(\omega) \\ S_{bs}(\omega) & S_{bb}(\omega) \end{bmatrix} \begin{Bmatrix} U_s(\omega) \\ U_b(\omega) \end{Bmatrix} = \begin{Bmatrix} F_s(\omega) \\ F_b(\omega) \end{Bmatrix} \quad (2)$$

$$\begin{bmatrix} M_{ss} & M_{sb} \\ M_{bs} & M_{bb} \end{bmatrix} \begin{Bmatrix} \ddot{u}_s(t) \\ \ddot{u}_b(t) \end{Bmatrix} + \begin{bmatrix} K_{ss}^* & K_{sb}^* \\ K_{bs}^* & K_{bb}^* \end{bmatrix} \begin{Bmatrix} u_s(t) \\ u_b(t) \end{Bmatrix} = \begin{Bmatrix} f_s(t) \\ f_b(t) \end{Bmatrix} \quad (3)$$

In the above equations, subscript  $s$  denotes structural region while  $b$  refers to the interface between the near and far fields.  $S_{ij}(w)$  are stiffness sub-matrices of the model; while  $S_{ss}$  refers to stiffness matrix of the structural and near field soil region;  $S_{sb}$  and  $S_{bs}$  are stiffness matrices of the interface between near and far field regions and finally  $S_{bb}$  is the far field stiffness matrix. The corresponding stiffness sub-matrices are complex in nature, *i.e.*  $K_{ij}^* = K_{ij}(1 + i\xi)$  where  $\xi$  is the material damping ratio. If the material damping is ignored for a region, the corresponding stiffness sub-matrix is real valued and the asterisk sign is removed from its notation.

The dynamic stiffness sub matrices of the far field soil region,  $S_{bb}$ , can be obtained using the infinite elements.  $U_s(\omega)$  and  $U_b(\omega)$  are the Fourier transforms of displacement and force vectors.  $u(t)$  and  $f(t)$  are the displacement and force vectors in time domain respectively, while  $F_b(\omega)$  and  $f_b(t)$  are the interaction force vectors of the interface between the near and far fields in frequency and time domains respectively. These are defined as

$$\begin{aligned} F_b(\omega) &= -S_{bb}^g(\omega)U_b(\omega) \\ f_b(t) &= -\int_0^t S_{bb}^g(t-\tau)u_b(\tau)d\tau \end{aligned} \quad (4)$$

In which  $S_{bb}^g(t)$  is the coefficient matrix of a response function resulting from a unit displacement impulse. It can be obtained by taking the IFFT of  $S_{bb}^g(\omega)$  as

$$S_{bb}^g(t) = IFFT(S_{bb}^g(\omega)) = \frac{1}{2\pi} \int_{-\infty}^{+\infty} S_{bb}^g(\omega)\exp(i\omega t)d\omega \quad (5)$$

## 2.1 Numerical modeling of SSI problems

Finite element analysis of geomechanical problems often presents difficulties in modeling unbounded domains of soil or rock. A common approach is the truncation of the far filed region and hence arbitrarily locating the boundaries which often results in significant errors in the computed solutions (Bagheripour and Marandi 2003, Bagheripour and Marandi 2005). However, use of a large number of finite elements to remove the boundary effects may be considered as a solution; however, this approach requires large computational time and resources which makes the analysis an unworthy practice. Additional difficulties arise from the reflection of waves off the artificially truncated boundaries which may lead to spurious results (Chuhan and Zhao 1987).

A wide variety of artificial finite boundaries and coupling techniques have been developed in the past to overcome these problems including viscous damping boundary (Lysmer and Kuhlemeyer 1969, White *et al.* 1977), superposition boundary (Cundall *et al.* 1978), wave transmitting boundary (Liao *et al.* 1984), consistent boundary (Kausel 1974), boundary elements (Wolf 1985) and even scaled boundary element (Baziar 2007). More recently, Deneme *et al.* (2008) investigated and compared some discontinuous boundary elements for 2D soil-structure interaction. Multipurpose computer program coded in Fortran 77 was developed for each type of boundary elements and for

elastic or visco-elastic 2D SSI problems. However, the discontinues boundary elements developed by Deneme *et al.* (2008) appears to be incapable of capturing the frequency dependant characteristics of soils. The purpose of these boundaries is to absorb the incoming waves so that they are not reflected off of the artificially truncated boundary and hence to model the real behavior of the domain. Wang (2005) discussed on the influence of different boundary conditions on analysis of SSI problems such as reactor buildings response using CALSSI and FLUSH computer codes. He concluded that in order to absorb, instead of reflect, the outwardly radiating energy, the use of transmitting boundary conditions at the soil-structure interface should be considered. In order to simulate the effect of the far field on the near field more intuitively and numerically, infinite elements (*e.g.* Bettles 1977) have been developed in recent years. Some numerical results (Chuhan and Zhao 1987, Zhao 1991) indicate that the coupling of finite and infinite elements (FE-IFE) is an effective framework to simulate wave propagation problems in infinite media. Using this method, not only the geometrical irregularities and geological complexities in the near field are simulated, but also the wave propagation characteristic of the system is effectively taken into account.

### 3. Finite element and infinite elements

In formulation of dynamic infinite elements, amplitude decay and phase delay of the wave propagation are taken into account. The shape functions of such element must reflect the far field characteristics; *i.e.* it must satisfy the radiation condition as well as the decay of state variables (*e.g.* displacements) to zero at infinity. Shape function of an infinite element which extends to infinity in  $\xi$  direction (Fig. 2) may be written as (Kim 1999, Yun *et al.* 2000)

$$N_j'(\xi, \eta) = N_j(\xi, \eta)e^{-ik\xi(\xi_1-\xi)/L} \tag{6}$$

where  $N_j(\xi, \eta)$  are the conventional element shape functions,  $k$  is the wave number of propagating wave and  $L$  is scaling length. The first exponential term in Eq. (6) represents the basic shape of the propagating wave while the second exponential term enables the variables to go to zero

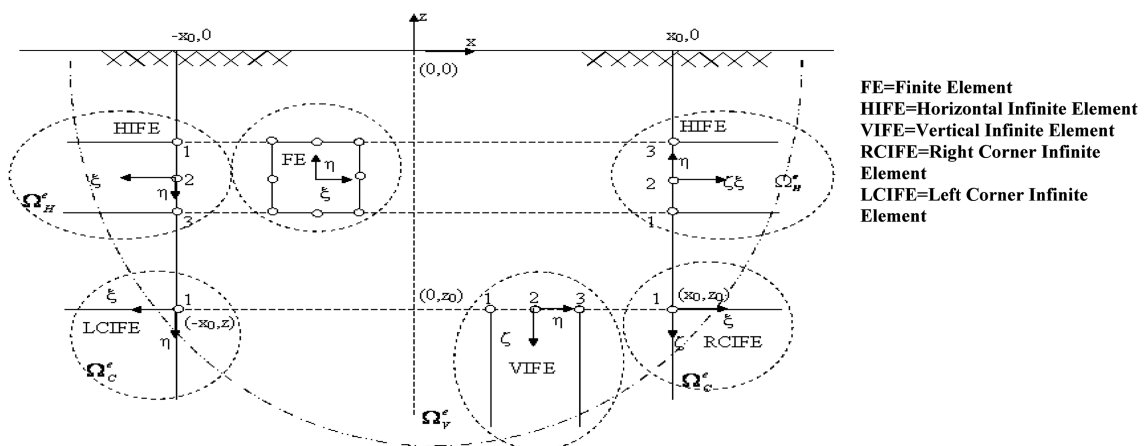


Fig. 2 Global and local coordinates adopted for the development of Finite Elements (FE) as well as Infinite Elements (IFE)

as  $\xi$  goes to infinity. A detailed discussion on the effects of length scale can be found in other published works (Kim and Yun 2000, Zhao and Zhang 1989). Element matrices are formulated in the usual way. The element stiffness and mass matrices are expressed in the form

$$[M]^e = \int_{-1}^1 \int_0^\infty [N]^T \rho [N] |J| d\xi d\eta \quad (7a)$$

$$[K]^e = \int_{-1}^1 \int_0^\infty [B]^T [D^*] [B] |J| d\xi d\eta \quad (7b)$$

Infinite element formulation considered in this paper clearly shows that frequency of the input is importance and are formulated in frequency domain. However, in order to use these elements in a time domain analysis, the frequency  $\omega$  should be fixed. Usually the predominant frequency of the input is considered for  $\omega$  (Kramer 1996) in order to reach the most significant response of the system under a given input motion. The infinite elements developed specifically for time domain analysis are essentially similar to static type of infinite elements (Bettes 1977) and does not include wave propagation characteristics such as  $k$ . The main advantage of the infinite elements developed in frequency domain is clearly the simplicity of the formulation particularly for amplitude attenuation terms. These terms guarantee the decay of wave energy as it occurs in real situations.

### 3.1 Mapping function and shape functions for IFE's

Mapping functions are used to relate the local coordinates ( $\xi, \zeta$ ) to the global coordinates ( $x, z$ ) and are defined for 3 types of infinite elements shown in Fig. 2. These are as follows

$$x = x_o(1 + \xi) \quad z = \sum_{j=1}^N L_j(\eta) z_j \quad \text{for HIFE} ((x, z) \in \Omega_H^e) \quad (8a)$$

$$x = x_o(1 + \xi) \quad z = z_o(1 - \zeta) \quad \text{for LCIFE or RCIFE} ((x, z) \in \Omega_{LC}^e \text{ or } \Omega_{RC}^e) \quad (8b)$$

$$x = \sum_{j=1}^N L_j(\eta) x_j \quad z = z_o(1 - \zeta) \quad \text{for VIFE} ((x, z) \in \Omega_V^e) \quad (8c)$$

where  $x_o$  and  $z_o$  are global coordinates of the corner points in the regions defined by  $\Omega_{LC}$  or  $\Omega_{RC}$  which are also shown schematically in Fig. 2.  $x_j$  and  $z_j$  are also the global coordinates at elemental node  $j$ .  $L_j(\eta)$  is a Lagrangian polynomial which has unit value at node  $j$  and zero at all other nodes. Here the local coordinates vary within the limits  $\xi \in [0, \infty]$ ,  $\zeta \in [0, \infty]$  and  $\eta \in [-1, 1]$ . Shape functions for infinite elements define a displacement field based on propagation waves into an infinite domain, *i.e.*

$$u(x, z, \omega) = \sum_{j=1}^N \sum_{m=1}^m N_{jm}(x, z, \omega) P_{jm}(\omega) \quad (9)$$

where  $P_{jm}(\omega)$  are the corresponding generalized coordinates and  $N_{jm}(x, z, \omega)$  are displacement shape functions.  $N$  is the number of nodes for horizontal and vertical infinite elements which also represents the number of horizontal wave functions for the left and right corner infinite elements (LCIFE and RCIFE).  $m$  is the number of shape functions considered in the formulation of infinite elements. The shape functions  $N_{jm}(x, z, \omega)$ , for all 3 types of infinite elements used here (also

shown in Fig. 2) are defined by

$$N_{jm}^H(\xi, \eta, \omega) = L_j(\eta) \exp(-C_m(\omega)x_o\xi) \quad \text{for HIFE} \quad (10a)$$

$$N_{mp}^C(\zeta, \xi, \omega) = \exp(-C_m(\omega)x_o\xi) \exp(-C_p(\omega)z_o\zeta) \quad \text{for LCIFE \& RCIFE} \quad (10b)$$

$$N_{jp}^V(\zeta, \eta, \omega) = L_j(\eta) \exp(-C_p(\omega)z_o\zeta) \quad \text{for VIFE} \quad (10c)$$

where  $C_m(\omega)$  and  $C_p(\omega)$  are defined as

$$C_m(\omega) \in \left\{ \begin{array}{l} \alpha + i\beta_1 \\ \alpha + i\beta_2 \\ i\beta_3 \end{array} \right\} \quad C_p(\omega) \left\{ \begin{array}{l} \alpha + i\beta_1 \\ \alpha + i\beta_2 \end{array} \right\} \quad (11)$$

where  $\alpha$  ( $0 < \alpha \leq 1$ ) and  $\beta_j$  ( $j = 1, 2, 3$ ) are the displacement amplitude decay factor and the nominal wave number in local coordinates of an infinite element respectively. In above relations, the general term  $\exp(-C_m(\omega)x, \xi) = \exp(-(\alpha + i\beta)x, \xi)$  may be decomposed into two separate terms of which the term  $e^{-\alpha\xi}$  expresses the amplitude attenuation due to wave dispersion while  $e^{-i\beta\xi}$  defines phase delay due to wave propagation in local coordinate system. The index  $j$  ( $j = 1, 2, 3$ ) for parameter  $\beta$  denotes the wave numbers for shear, compression, and Raleigh waves respectively. In formulation of the infinite element studied here, the Rayleigh wave components are not included for the vertical and the corner infinite element since these components decay quickly as depth increases.

### 3.2 Near field stiffness and mass matrices for structure and soil domain

Near field includes the structure and a limited area of the soil region surrounding the structure which is modeled mainly by finite elements. For this purpose a 4-node plane isoparametric element formulation is used. Stiffness and mass matrices for these elements are calculated based on Gauss integration rules and are not repeated here (Chuhan and Zhao 1987, Kim and Yun 2000, Zhao and Valliappan 1992). A 2D frame element is used to model the structure. For this purpose an element with 3 degrees of freedom at each joint is introduced and then stiffness, mass and damping matrices are formed using standard finite element procedures (Logan 2008).

## 4. Solving the differential equation of motion by HAAR wavelet

### 4.1 A brief review on the Wavelet Theory (WT)

Wavelet theory has been successfully applied in the analysis of complex and random input waves in many engineering disciplines. In summary, WT is a mathematical transformation which is applied to signals such as an accelerogram output to obtain further information from that signal that is not readily available in the raw data. There are, however, a number of transformation schemes that can be applied, among which the Fourier Transform (FT) is probably by far the most popular. In an FT analysis, a signal like an accelerogram is decoupled into a series of harmonic waves with amplitude and frequencies which are determined. However, the problem with such analysis is that the specific

time at which a given harmonic wave occurs cannot be determined in FT. This, however, can be easily performed by a WT analysis. The differences between the Fourier transform (FT) and Wavelet Transform (WT) are as follows:

A- In FT, the harmonic waves (extracted from the original wave) have no time limits and they essentially contribute to the original wave from  $-\infty$  to  $+\infty$ . Wavelets, on the other hand, have limited length in both time and frequency domain.

B- In FT, harmonic waves are predictably regular, symmetric, and flat while in WT these waves may be irregular and asymmetric.

C- Original waves (especially those of earthquake records) often have sudden and drastic changes in very short period of time. WT have better compatibility with such sudden or drastic changes and better approximates the extremes of the original waves.

D- Since the wavelets have limited time spans, the investigation on a particular part of the original wave, which may have limited time duration, is more easily implemented.

Application of wavelet theory in analysis of structural response to earthquake loading has been considered by some researchers in the past (Heidari 2004, Lepik 2004). However most of these applications are limited to approximation of earthquake wave's acceleration data by reducing the number of sampling points. Another useful aspect of the wavelet theory is that it offers a special technique of solving time dependent differential equations. Furthermore, in complex engineering problems such as SSI analysis, wavelet theory reduces the problem into a number of separate and more manageable parts which can be easily be combined together again to recover the total response of the problem. In context of signal processing and engineering problems, various types of wavelets have been introduced in the literature by many researchers. The description of all will lead to a lengthy discussion and is not the scope of this paper. Amongst them, Harr wavelet is considered the most suitable one for the SSI analysis conducted here and especially for solution of differential equation of system (Lepik 2004).

#### 4.2 Haar wavelet

There is no derivation in non-continuous nodes of Haar wavelet. It makes the concept non-applicable directly to solution of differential equations. However, this can be overcome by the integral method in which the upper degree of derivation in equation should be expanded. Chen and Hsiao (1997a, 1997b) described a method of transferring a differential equation into an algebraic equation. The method is often referred to as the Chen and Hsiao Method (or CHM).

In this paper equation of motion is solved by Haar wavelet. Cattani (2004) proposed a complementary segmentation approach into the Harr wavelet in which the complexity of calculations is reduced. This is also referred to as Segmentation Method or simply SM. Further simplification into the Harr wavelet has been introduced by Goedecker and Ivanov (1998) and Hsiao and Wang (2001) in which upper degree of derivation is assumed constant at each segment leading to a much less complicated approach. It is also known as Piecewise Constant Approximation (PCA) method. These simplifications have been taken into consideration in current study. Fig. 3 schematically shows the Haar orthogonal functions.

If the square of a function  $y(t)$  can be integrated and its integral is bounded, then it can be expanded by Haar wavelet (Chen and Hsiao 1997a)

$$y(t) = c_0 h_0(t) + c_1 h_1(t) + c_2 h_2(t) + \dots \quad (12)$$

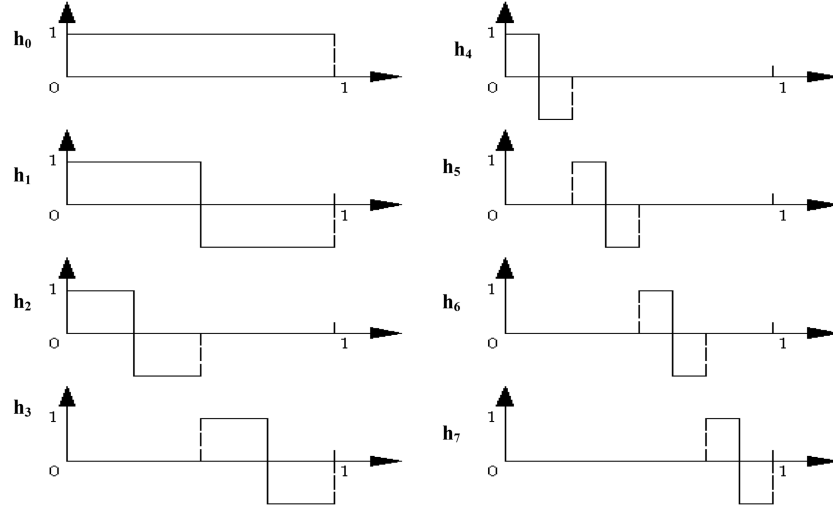


Fig. 3 Haar wavelet and its integrals

in which

$$c_i = 2^j \int_0^1 y(t) h_i(t) dt \quad (13)$$

### 4.3 Solving the equation of motion

The second order differential equation of motion with dependent variable  $u$  is as follows

$$\frac{d^2 u}{dt^2} = F\left(t, u, \frac{du}{dt}\right), t \in [0, T] \quad (14)$$

In order to find a proper solution, the following set of first order equation is considered as an alternative to the Eq. (14)

$$\frac{du}{dt} = v, \frac{dv}{dt} = F(t, u, v) \quad (15)$$

The time span is divided into  $N$  parts and length of the  $n^{\text{th}}$  segment is shown by  $d_n$ . To use Wavelet Transform (WT) the local time is shown as

$$\tau = \frac{t - t_n}{d_n} \quad (16)$$

Eq. (15) in local time is shown as below

$$\dot{u} = d_n v, \dot{v} = d_n F(t_n + d_n \tau, u, v) \quad (17)$$

Variables  $\{u\}$  and  $\{v\}$  are considered vectors with corresponding components as  $u_j = u(\tau_j)$ ,  $v_j = v(\tau_j)$ ,  $j = 1, 2, \dots, 2M$ . In first order Eq. (17), the derivation part is expanded by Haar series.

$$\dot{u} = aH, u = aPH + u_n E \quad (18a)$$

$$\dot{v} = bH, v = bPH + v_n E \quad (18b)$$

In Eq. (18),  $a$  and  $b$  are vectors such that  $a^T$  and  $b^T$  become vectors with  $2M$  columns.  $E$  is a unit vector with  $2M$  columns and  $u_n, v_n$  are values of  $u$  and  $v$  over the boundary condition at  $t = t_n$ . By substituting Eq. (17) into Eq. (18),  $aH$  and  $bH$  are rewritten as follows

$$bH = d_n F(t_n + d_n \tau, aPH + u_n E, bPH + v_n E) \quad (19a)$$

$$aH = d_n (bPH + v_n E) \quad (19b)$$

Vectors  $a$  and  $b$  are calculated by the matrix equations defined above while  $u$  and  $v$  are obtained from Eq. (18).

In order to solve the next part,  $u_{n+1}$  and  $v_{n+1}$  should be calculated such that

$$u_{n+1} = a_1 + u_n E, v_{n+1} = b_1 + v_n E \quad (20)$$

where  $a_1$  and  $b_1$  are the first components of  $a$  and  $b$  vectors.

Eq. (20) clearly shows that displacement components ( $u, v$ ) at any step is related to the corresponding values of the displacement component at pervious step. In other words  $u_{n+1}$  and  $v_{n+1}$  are related to  $u_n$  and  $v_n$  correspondingly.

#### 4.4 Solving equation of motion for multi degree of freedom

Equation of motion with  $n$  degrees of freedom is expressed in time domain as

$$[M]\{\ddot{u}\} + [C]\{\dot{u}\} + [K]\{u\} = \{f(t)\} \quad (21)$$

In above equation,  $[M]$ ,  $[C]$ ,  $[K]$  are the mass, damping, and stiffness matrices respectively. In order to solve this equation by the method presented here, it is arranged as follows

$$\{\ddot{u}\} = [M]^{-1} \{ \{f(t)\} - [C]\{\dot{u}\} - [K]\{u\} \} \quad (22)$$

The following equations are also developed in a similar manner for a single degree of freedom system. In other words

$$\{\dot{u}\} = d_n \{v\} \quad (23)$$

$$\{\dot{v}\} = d_n [M]^{-1} (\{f(t)\} - \{C\}\{\dot{u}\} - \{K\}\{u\}) \quad (24)$$

To solve this system, PCA method is adopted. The method necessitates that  $H = 1$  and  $P = 0.5$  be adopted. Then,  $a_n$  and  $b_n$  are obtained by substitution of Eqs. (23) and (24) into Eq. (18) which leads to the following relation

$$\{a_n\} = \frac{0.5d_n^2 \{f(t_n)\} - 0.5d_n^2 [K]\{u_n\} + d_n [M]\{v_n\}}{0.25d_n^2 [K] + [M] + 0.5d_n [C]} \quad (25)$$

$$\{b_n\} = \frac{d_n \{f(t_n)\} - d_n [C]\{v_n\} - d_n [K]\{u_n\} - 0.5d_n^2 [K]\{v_n\}}{0.25d_n^2 [K] + [M] + 0.5d_n [C]} \quad (26)$$

To reach the final solution, Eqs. (25) and (26) should be substituted into Eq. (20) to yield

$$\{u_{n+1}\} = \frac{0.5d_n^2\{f(t_{n+1})\} + d_n[M]\{v_n\} - 0.25d_n^2[K]\{u_n\} + [M]\{u_n\} + 0.5d_n[C]\{u_n\}}{0.25d_n^2[K] + [M] + 0.5d_n[C]} \quad (27)$$

$$\{v_{n+1}\} = \frac{d_n\{f(t_{n+1})\} - d_n[K]\{u_n\} - 0.25d_n^2[K]\{v_n\} - 0.5d_n[C]\{v_n\} + [M]\{v_n\}}{0.25d_n^2[K] + [M] + 0.5d_n[C]} \quad (28)$$

Parameters  $a_n$  and  $b_n$  are calculated based on Eqs. (25) and (26) at any given step which are combined with  $u_n$  and  $v_n$  through Eq. (20). This procedure is a repetitive concept which is started from step ( $n=0$ ) one and is progressively repeated to the last step ( $n=N$ ) where  $N$  is the maximum number of time step. It should be mentioned that in developing such a stepwise procedure, the boundary conditions  $u_0=0$  and  $v_0=0$  are defined. At each step, Eqs. (25) and (26) are solved. The resulting  $a_n$  and  $b_n$  are subsequently used for solving Eqs. (27) and (28). This time marching ultimately develops the time domain response.

## 5. Numerical examples and validation of the proposed concept

### 5.1 Example 1

In order to investigate the accuracy of computed solution obtained using wavelet theory, a typical structural earthquake analysis is conducted on a 5 storey framed structure with a span of 5 meters subjected to El Centro earthquake record. All structural members are adopted as IPB300 and for sake of simplicity, no SSI analysis is considered at this stage and common fixed supports are used at structure's base. The WT solution is compared with those obtained by other conventional methods such as Wilson- $\theta$  procedures. Comparison of the results given by both methods is shown in Fig. 4 which demonstrates good agreement and accuracy for results obtained by WT.

### 5.2 Example 2

The example considered in this section is designed to demonstrate the applicability and efficiency

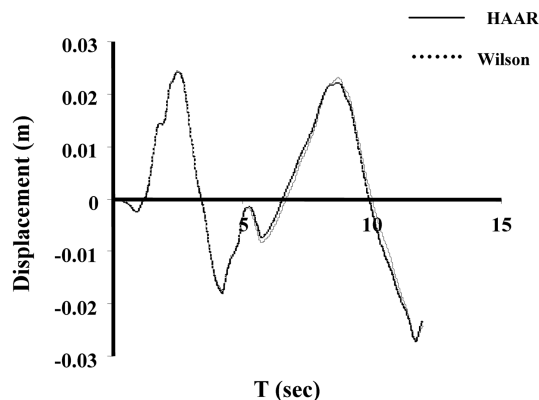


Fig. 4 Comparison between the results obtained for the Example 1

Table 1 Structural and foundation properties adopted in the numerical Example 2

Element	Structural properties				Property	Foundation properties		
	Beams		Columns			Concrete	Soil	Bed rock
Properties	2IPE240	BOX(1)	BOX(2)	BOX(3)	$H$ (m)	0.8	40	–
$I_x = I_y$ ( $\text{cm}^4$ )	7780	19143	10812	7566	$\rho$ ( $\text{t/m}^3$ )	2.4	1.89	2.65
$A$ ( $\text{cm}^2$ )	28.6	138.27	114.24	77.44	$V_s$ (m/s)	2050	502	3160
$H$ (cm)	24	30	25	25	$E$ ( $\text{KN/m}^2$ )	24E6	3.3E5	29.2E6
$\gamma$ ( $\text{KN/m}^3$ )	78.5	78.5	78.5	78.5	$\xi$	0.02	0.05	0.02
$E$ ( $\text{KN/m}^2$ )	20.4 E6	20.4 E6	20.4 E6	20.4 E6	Comment:			
$\xi$	0.02	0.02	0.02	0.02	Box(1) = 30×30×1.2 (cm)			
					Box(2) = 25×25×1.2 (cm)			
					Box(3) = 25×25×0.8 (cm)			

of the approach proposed here in this paper. Seismic response and SSI analysis of a 10 storey building slightly embedded in a soil layer overlaying a rock formation is presented using 3 different approaches including the one proposed in this paper. Results are compared and discussions are provided. Geometrical and mechanical properties of the soil layer used here are summarized in Table 1 in conjunction with structural elements properties. Total height and width of the building are 32 m and 12 m respectively. In SSI analysis, system under study including the soil layer and the structure is subjected to an acceleration time history of Naghan earthquake recorded in the past. The main accelerogram data for Naghan earthquake is shown in Fig. 5 while the Fourier spectrum obtained by FFT procedure (Fast Fourier Transform) is depicted in Fig. 6. The procedure was carried out by a computer program coded in FORTRAN 77 developed by authors; however, it may be implemented also by other available softwares such as MATLAB or by TSPP computer program (Boore 2008). Considering the fact that soil layer beneath the structure has a thickness of about 40 m, then the fundamental frequency for the soil layer is evaluated as  $\omega_1 = \pi V_s / 2H \approx 19$  rad/sec which is close to the predominant frequency depicted in Fourier spectrum. In fact, the thickness of soil layer has been deliberately selected as such value ( $H = 40$  m) so that near resonance condition are created for the soil layer thereby creating the largest possible interaction effects under the given base motion (in this example Naghan earthquake record). To demonstrate the interaction effects, results obtained here are first compared to those obtained for a conventional fixed support structure. Next, results of the current SSI approach are further compared to those obtained from other SSI models.

### 5.2.1 Comparison of the current SSI concept with conventional fixed support analysis

To show the significance of SSI effects and to establish a basis for comparison, it is necessary to conduct a conventional fixed support structural analysis in which the seismic interaction effect is neglected. Such an analysis is usually conducted by common structural analysis softwares like ANSYS or PLAXIS (Brinkgreve *et al.* 1988). Fig. 7 shows the discretized and FE structural model generated using ANSYS commercial software where fixed nodes are defined at the base of the model. Seismic response of the structure subjected to Naghan earthquake acceleration record is shown in Fig. 8a, b. A study on the maximum displacement and the induced base shear force to the structure is conducted. It can be seen from this figure that the maximum displacement of rigid base

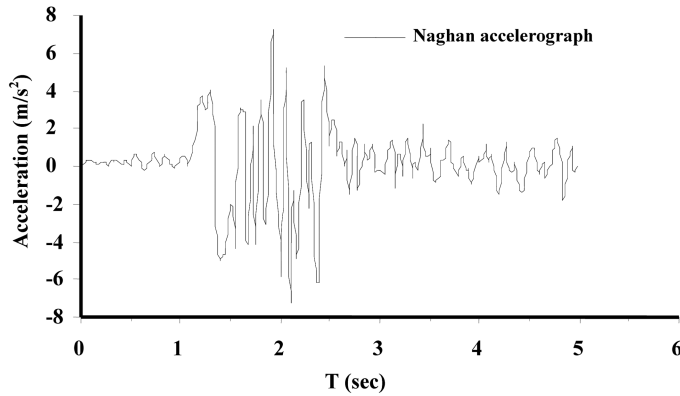


Fig. 5 Input Naghan acceleration time history

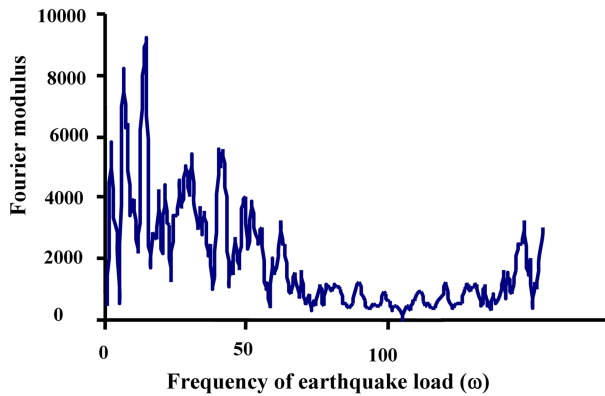


Fig. 6 Fourier spectrum

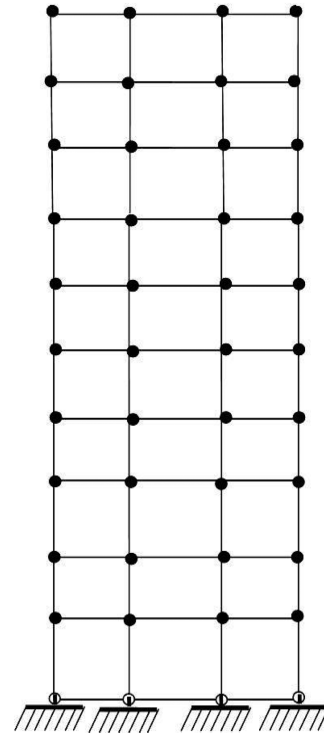


Fig. 7 FE model for fixed support structure studied in Example 1

structure reaches 57 cm. The figure also shows that the structure undergoes a maximum base shear force of about 1.47 MN.

The SSI model based on the FE-IFE concept developed in this study is shown in Fig. 1(b). The figure also shows the locality of all three types of infinite elements used to model the boundaries. In order to establish a comparison base and to emphasis on interaction effects, the earthquake record used in the analysis of fixed support structure is applied to the current SSI model. The displacements and base shear forces verse time are shown in Fig. 9(a) and (b). From this figure, it can be seen that maximum displacement of the structure is about 30 cm while the base shear force is slightly higher than 650 KN. Comparing the results shown in Fig. 9 to those obtained for the rigid base structure (Fig. 8) reveals that maximum displacement of the structure has been reduced, mainly due to interaction effects. In fact, since the soil acts as a flexible medium, it undergoes deformation and hence the relative deformation of the structure is reduced. Infinite elements defined along the model's boundaries allows the seismic waves to dissipate and prevent them from reflecting as is mostly the case in common FE models.

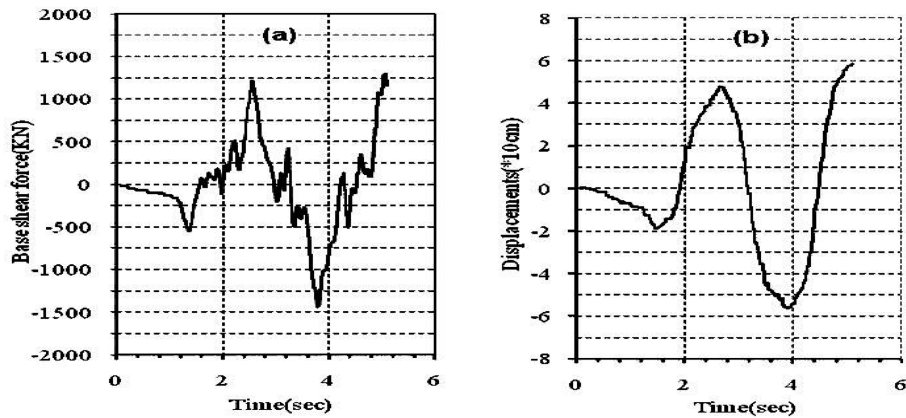


Fig. 8 Seismic response of the structure subjected to Naghan earthquake record: (a) Base shear force, (b) Displacements

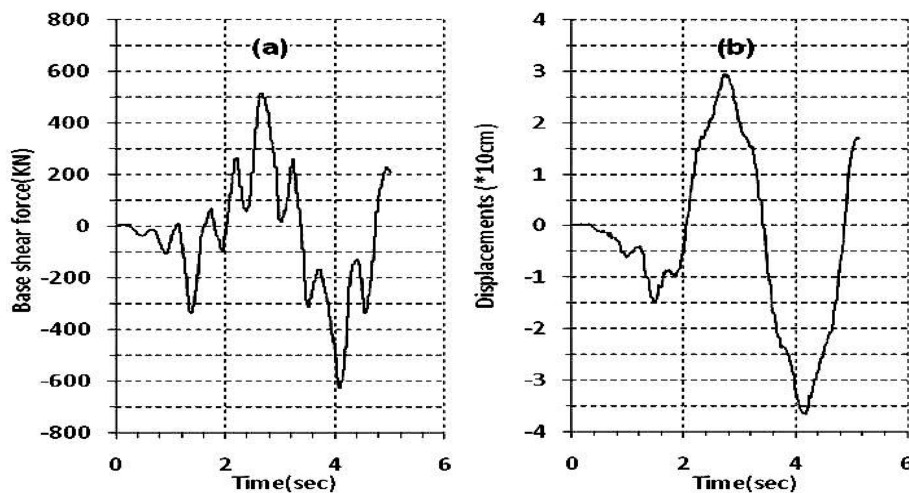


Fig. 9 Response of the model subjected to Naghan earthquake record considering SSI effect: (a) Base shear force, (b) Displacements

### 5.2.2 Comparison of the results with other SSI methods

Two other available SSI methods are used to compare the results obtained from the proposed method. They are a) Sub structuring method and b) Direct method using extensive FE mesh to model soil region. ANSYS 5.4 engineering software is used to develop the FE model for these two concepts which are shown in Figs. 10 and 11.

### 5.2.3 Comparison with substructure method

In sub structuring approach the entire system of soil and structure is broken down into separate parts as shown in Fig. 12. The equation of motion for the whole system shown in Fig. 12 can be expressed as

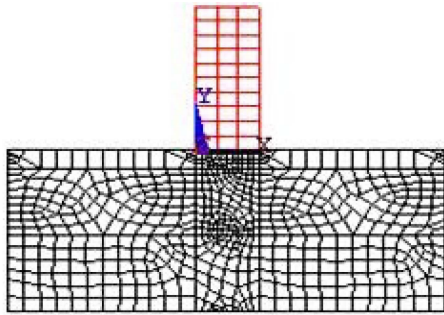


Fig. 10 FE extensive mesh for direct SSI analysis

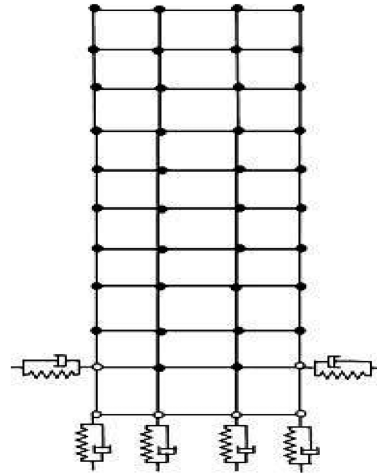


Fig. 11 Scheme of the structural model supported on fictitious spring and dashpots developed for sub structuring SSI analysis

$$[M_t]\{\ddot{u}\} + [C_t]\{\dot{u}\} + [K_t]\{u\} = \{P\} \tag{29}$$

where  $[M_t]$ ,  $[C_t]$ , and  $[K_t]$  are the total mass, damping, and stiffness matrices while  $\{P\}$  is the vector of exciting force. These matrices are further defined as

$$[M_t] = [M_n] + [M_f] \quad [C_t] = [C_n] + [C_f] \quad [K_t] = [K_n] + [K_f] \tag{30}$$

in which subscripts  $n$  and  $f$  represent the near and far field respectively.

There are two main steps in sub structuring technique as applied to SSI analysis are: 1) determination of the free field motion under a given strong base motion, 2) evaluation of dynamic

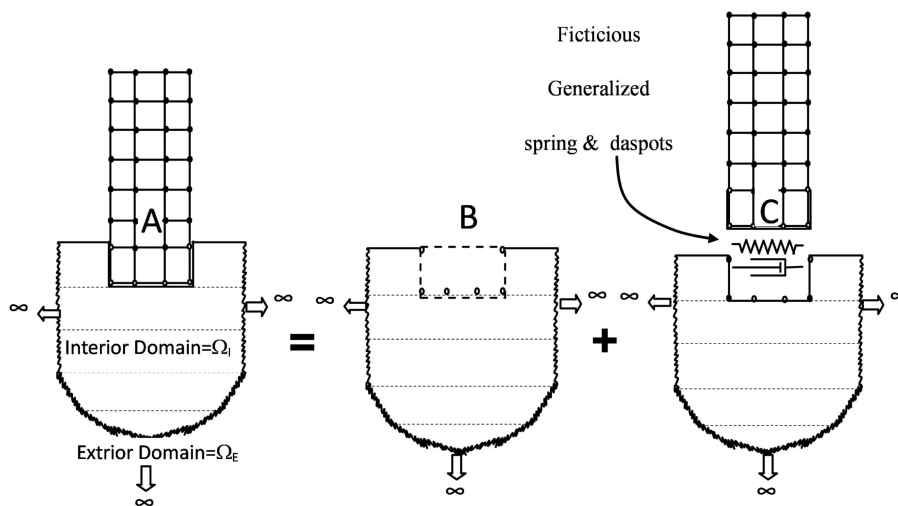


Fig. 12 Concept of sub structuring for SSI analysis discussed in Example 2

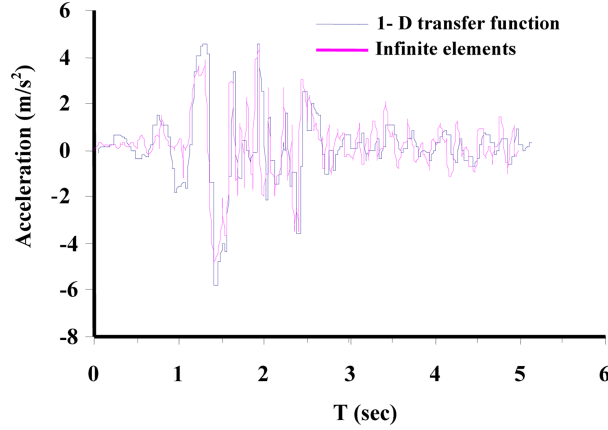


Fig. 13 Acceleration at soil surface obtained by FE-IFE and analytical approach

impedance and stiffness coefficient of the soil foundation which are essentially frequency dependant. In such a general approach, the dynamic stiffness coefficients of the soil region can physically be interpreted as a generalized spring-dashpot system. Thus, SSI analysis is carried out for the structure supported on a series of spring-dashpot systems (Fig. 11) and for a loading case which depends on the free field motion determined in step 1 (Wolf 1985, Bagheripour and Marandi 2005, Gouasmia and Djeghaba 2007). Here the loading case is in fact the motion of the soil surface; that is obtained using special transfer functions and commonly results in a transferred accelerogram (Kramer 1996). For the example under study, this is shown in Fig. 13. For sake of comparison, the surface accelerogram is also obtained using FE-IFE methodology discussed in this paper; and it superimposed on the Fig. 13. The main stages of SSI analysis as related to calculation of free field response of the soil layer and determination of soil dynamic impedance as well as calculation of the generalized fictitious springs and dashpots are completely carried out in frequency domain using complex valued parameters; and by means of FE-IFE technique (Zhao *et al.* 1991).  $K_e$  and  $C_e$  for the soil region, *i.e.* far field, are evaluated through the calculation of impedance function matrix of the far field. If the far field is modeled by infinite elements for a given frequency, say  $\omega$ , the decoupled equation of motion for only the far field is defined as

$$[-\omega^2[M_f] + i\omega[C_f] + [K_f]]\{u_f(\omega)\} = \{p_f(\omega)\}$$

or

$$\overline{[K_f(\omega)]}\{u_f(\omega)\} = \{p_f(\omega)\} \quad (31)$$

where subscript  $f$  denotes the far field and  $[M]$ ,  $[C]$ ,  $[K]$  represent the mass, damping and stiffness matrix respectively. In such solutions the displacements and forces are of a complex form, thus

$$\{u_f(\omega)\} = u_1 + i.u_2 \quad \text{and} \quad \{p_f(\omega)\} = p_1 + i.p_2 \quad (32)$$

The load-displacement relation is again defined in a complex form as

$$\overline{[K_f(\omega)]} = [K_1(\omega)] + i.[K_2(\omega)] = \frac{\{p_f(\omega)\}}{\{u_f(\omega)\}} \quad (33)$$

Table 2 Coefficients of the springs and dashpots obtained by FE-IFE technique

Property/Direction	Horizontal	Vertical
$K_e$ (KN/m)	113500	165800
$C_e$ (KN.Sec/m)	0.370	0.038

in which  $\overline{[K_f(\omega)]}$  is, in fact, the dynamic impedance matrix of the far field of the system. It is seen that both the  $[K_1(\omega)]$  and  $[K_2(\omega)]$  are functions of the exciting frequency which constitute imaginary parts of the total stiffness matrix respectively. The total equivalent stiffness matrix of all fictitious generalized spring  $[K]_e$  and the equivalent damping matrix of all fictitious generalized dashpots  $[C]_e$  in the system can be defined as

$$[K]_e = [K_1(\omega)] \quad [C]_e = 1/\omega[K_2(\omega)] \quad (34)$$

Coefficients of springs and dashpots obtained by FE-IFE technique are summarized in Table 2. Time domain SSI analysis was conducted using ANSYS 5.4 software for the structure supported on generalized fictitious springs and dashpots. The corresponding FE model developed by ANSYS 5.4 is shown in Fig. 11. In Fig. 14 the structure response obtained using sub structuring approach is shown and is compared to that resulted from current method. Beside a small time phase, there is good agreement between the results obtained from these two methods.

Note here that in the case of high geometrical irregularity and material diversity in soil region, analytical solutions do not exist and hence the analysis of free field motion is only possible through a comprehensive computational approach such as FE-IFE concept.

#### 5.2.4 Comparison with direct time domain SSI analysis using extensive mesh

Unlike the sub structuring approach, the direct method involves establishing a computational

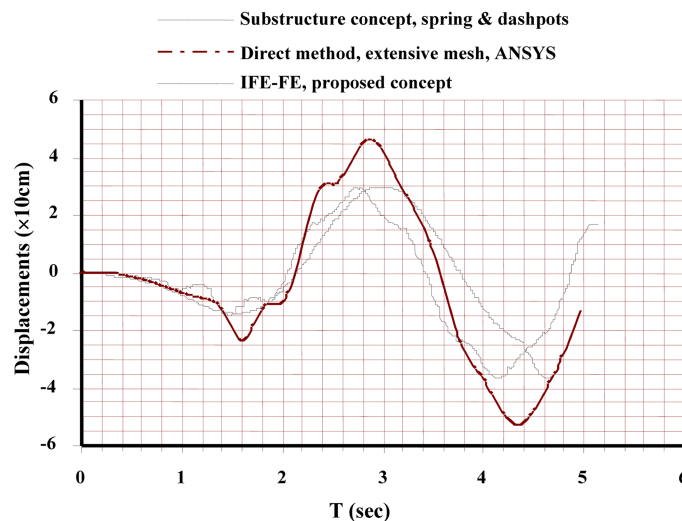


Fig. 14 Comparison of the SSI results obtained by proposed method (IFE-FE) with those given by two other concepts

model of the soil and the structure as a whole and analyzing it in one single stage. Here, there is no concept of boundary extension infinite elements; rather conventional nodal constrained are imposed at fictitious such models, Fig. 10, require extensive FE meshing in order to minimize the effect of the wave reflection produced by the boundaries and hence avoiding spurious solutions. In fact, the use of such extensive FE models is inevitable as they are needed to guarantee a degree of accuracy.

Plane finite elements were used to model the soil region while the structure itself is modeled using common beam and column elements. Assemblage of these two types of elements yields the total FE mesh which is then subjected to ground motion at the base. The response of this system to Naghan earthquake record is computed using ANSYS 5.4 engineering software. The response obtained is graphically superimposed, Fig. 14, where the results obtained by the other two SSI methods described in previous sections are also shown. It can be seen that amongst the three methods investigated here, the direct method predicts larger displacements for the structure despite the extensive mesh employed for the analysis. Perhaps to reach a better agreement with the current SSI approach and also with the sub structuring method, even larger FE mesh would have to be introduced. However, this would demand to an unacceptable level of time and resources which makes the method impractical. The sub structuring method and the current SSI approaches appear to be in good agreement. However, the current approach is advantageous since there is no need for the extra steps of free field analysis and determination of fictitious spring dashpot system.

### 5.3 Example 3: Response spectrum analysis with SSI effects using the proposed concept

A response spectrum analysis was conducted for this example and the impact of SSI was investigated. Here special consideration is given to the analysis of a simple one storey framed structure resting on the soil for which some building code design requirements are also available. The SSI effect was investigated for different soil types having various elasto-dynamic characteristics. In particular, the four types of soils that are defined in Iranian Building Code 2800 are adopted in this study; they correspond to the four types of soils defined by NEHRP codes as characterized in Table 3. Weight and base area of the foundation as well as the moment inertia of the foundation are calculated roughly as  $W = 100$  tons,  $A_0 = 8 \text{ m}^2$ , and  $I = 11 \text{ m}^4$  respectively. Also in Table 3 a summary of the calculated parameters required in the analytical response analysis based on period of structure and the modified period considering SSI effect are shown.

It can be seen from the Table 3 that SSI effects change structure's period. In fact, the softer the

Table 3 Soil properties and fundamental periods for structure studied in Example 3

Soil type		Parameters for analytical calculation of periods of the structure studied in Example 3								
Iranian building code (2800)	NEHRP	$\gamma$ (KN/m <sup>3</sup> )	$\alpha$	$V_0$ (m/s)	$G_0$ (MPa)	$V_s/V_0$	$G/G_0$	$V_s$ (m/s)	$G$ (MPa)	$\bar{T}/T$
I	B	22	1.894	1200	3168	0.7	0.49	840	1552.3	1.009
II	C	21	1.984	560	658.6	0.7	0.49	392	322.7	1.045
III	D	18	2.315	275	136.125	0.7	0.49	192.5	66.7	1.201
IV	E	17	2.451	150	38.25	0.7	0.49	105	18.7	1.605

soil is underneath the structure, as shear wave velocity reduces, the less is the total stiffness of the system. On the other hand, as the structure itself becomes less stiff, its original period is increased leading to a smaller ratio of  $\bar{T}/T$  irrespective of the soil types,  $T$  is the fundamental period of the structure which is characteristics of the structure and is calculated considering the mass and stiffness characteristics of the structure and based on the conventional fixed based analysis. However, due to the SSI effect, which is the matter of investigation in this paper, the period of the structure is changed which is shown by  $\bar{T}$ . Therefore, the symbol  $\bar{T}/T$  is, in fact, the ratio of these calculated periods.  $G$  and  $G_0$  refer to the shear modulus of the material which are soil and rock types. The shear stress-strain relation for soil materials are often regarded as “nonlinear elastic”. Hyperbolic model is one of the well known relations introduced in the context of geotechnical earthquake engineering which defines a nonlinear relation generally as  $G/G_0 = f(\gamma)$  where  $\gamma$  is the shear strain.  $G_0$  is a reference value for the shear modulus of the soil material, here in this paper soil types I-IV, which is obtained empirically in low shear strains. However,  $G$  is the value of shear modulus at any given level of shear strain which is calculated by empirical models such as Hyperbolic functions. In order to avoid complexity of the solution procedure, especially SSI analysis conducted in this paper, appropriate value of  $G/G_0$  at the limit of shear strain is adopted such that the superposition principle in the elastic range is sustained throughout the SSI analysis. Usually in deeper layers of a stratified soil system,  $G_0$  and  $V_0$  are increased when compared to those of the surfacial layers. This increase is attributed to the increase in stiffness of deeper layers. Interested reader may note that the soil system adopted for the analysis in Example 3 is not layered. In summary, for  $G/G_0$  and  $V_s/V_0$  constant values have been adopted since we are essentially dealing with a non-layered soil system under the structure.  $V_0$  is the shear wave velocity in soil or rock material at low shear strain while  $V_s$  is the velocity at any given shear strain.  $V_0$  and  $V$  can be related to  $G_0$  and  $G$  correspondingly by the following relations

$$G_0 = \rho V_0^2 \quad (35)$$

$$G = \rho V_s^2 \quad (36)$$

It can be concluded; from the discussion given above, that  $V_0$  and  $V$  are also strain dependants ( $\rho = \text{const.}$ ).

Similar to the  $G_0$  and  $G$ , one can regard the  $V_0$  as a reference value for  $V$ .

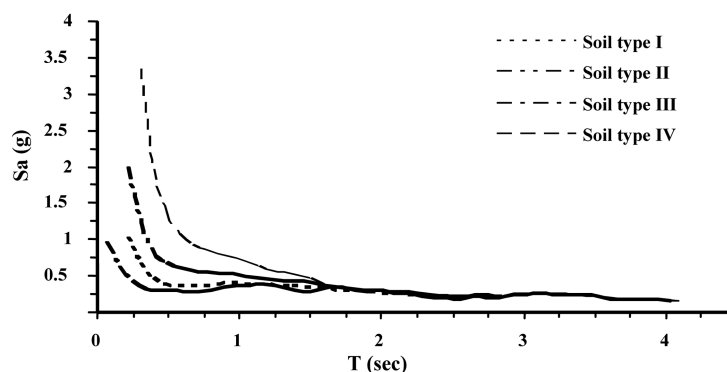


Fig. 15 Acceleration response spectrum for the structure studied in Example 3 subjected to El Centro earthquake using current SSI approach

In Fig. 15 the response spectrum for El Centro earthquake is developed using the presented method. The figure shows acceleration response spectrum obtained for the structure resting on soil types I to IV. However, the damping ratio is the same for all cases and is adopted as 5%. For other typical damping ratios of 2%, 10% and 20%, similar trends are observed for which the results are not included in this paper. For sake of comparison, the acceleration response spectrum developed for the conventional fixed based structure having various damping ratios (*i.e.*  $\xi = 0.02$  to 0.2) are also computed and shown in Fig. 16. Figs. 15 and 16, show that the structural response varies when considering the soil-structure interaction effects. These variations depend on soil type and rigidity of the structure. For soft soil with a stiff structure resonance will happen in lower periods.

Fig. 17 shows normalized spectral response of structure resting on either of the four soil types defined before, while SSI effects are taken into account. In developing curves in Fig. 17, the damping ratio was adopted as  $\xi = 0.05$  since Iranian Building Code 2800 also adopts a typical value of  $\xi = 0.05$  in development of design spectrum curves. Normalized spectral response developed for the conventional fixed based structure has also been superimposed in graphs of Fig. 17 for better comparison. It is seen from Fig. 17 that in structures with relatively low periods (say  $0.04 < T < 0.5$  sec) structural response depends significantly on soil type. Nevertheless, effect of soil types is also apparent from the figure which shows that for softer soils the difference between responses is

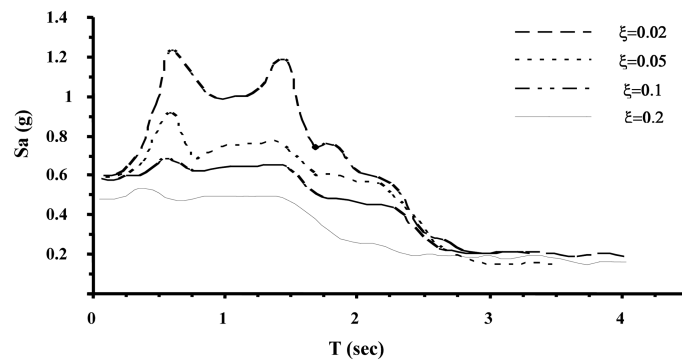


Fig. 16 Acceleration response spectrum for the structure studied in Example 3 subjected to El Centro earthquake using common fixed based analysis (no SSI effect)

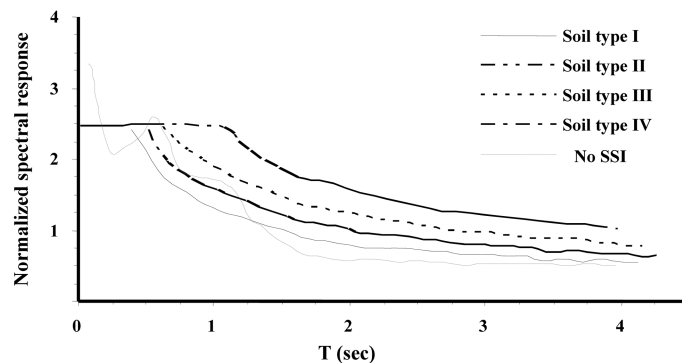


Fig. 17 Design spectrum of Iranian building code 2800 recommended for four soil types compared with conventional fixed based normalized response (no SSI)

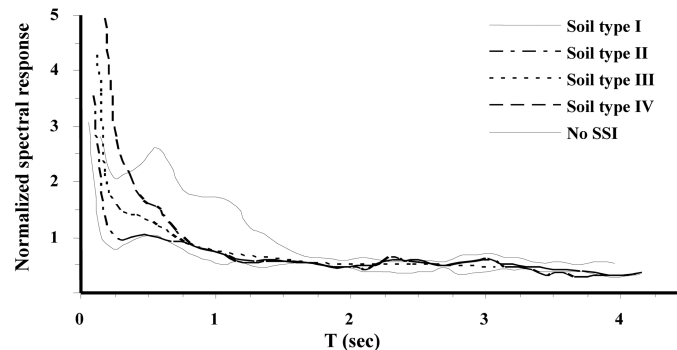


Fig. 18 Normalized spectral response of the structure studied in Example 3 resting on soil types I to IV compared with that of common fixed based structure (no SSI)

reduced. For structures with longer periods, the response becomes less dependant on the soil types and hence on the type of analysis (*i.e.* either with or without SSI effects). It can be generally concluded that as the soil becomes softer or the fundamental period of the structure increases, effects of SSI become less significant and the results obtained from either analysis, *i.e.* with or without SSI effects converge. Finally, the design spectrum recommended by Iranian Building Code 2800 is also compared with those neglecting SSI effects and are shown in Fig. 18. It can be deduced from this figure (also from other similar graphs developed for other earthquake records) that for periods lower than 0.35 sec, acceleration response obtained from the conventional fixed based structure (*i.e.* no SSI effect) is relatively higher than at predicted by Iranian Building Code 2800. This is an important issue in relatively tall buildings. For example, for a 5 storey building with fundamental period of 0.2 sec, the predicted response coefficient from a fixed based model (no SSI effects) is about 2.3 while for the same structure resting on either one of the four soil types; the building code considers a constant response coefficient of 2.5.

Very recently, Tabatabaifar and Massumi (2010) investigated the effect of SSI on RC-MRFs using a direct method. They discussed that for buildings higher than three and seven stories on soils with  $V_s < 175$  m/s and  $175 < V_s < 375$  m/s respectively, the SSI analysis for seismic design is essential.

## 6. Conclusions

A computational method based on coupled finite and dynamic infinite elements (FE-IFE) was presented to better model the soil-structure system and was applied to earthquake response analysis of structures. SSI analysis presents significant challenges, especially the extension of domain, boundary conditions, and determination of impedance functions as well as the evaluation of free field motion of the soil medium. An efficient way and integrated solution to these important issues is the use of infinite elements in modeling the soil region. Advantages of the approach are substantial reduction in degrees of freedom involved in the analysis and hence reduction in computational time and resources as well as increased efficiency without sacrificing accuracy. Another advantage of the proposed methodology presented here is that the dynamic system including the soil and structure is solved by wavelet theory (WT). This makes the concept presented even more efficient since in a detailed analysis, with access to both time and frequency domains,

more information on the response of a system can be obtained. The equation of motion is derived numerically for discretization of the soil domain. Formulations of the dynamic infinite elements were also presented in this paper.

The accuracy of the method presented here was examined by investigating typical structural models including single and multistory buildings. First the accuracy of WT approach was examined through earthquake response analysis of a multistory building. Good agreements were observed with Wilson- $q$  method. In another example studied, the initial results demonstrate that structural response is decreased due to soil interaction effects. While further comparisons revealed that the results of proposed method agree well with the sub structuring technique. However, due to the introduction of fictitious boundaries, the results of alternative models such as that comprised of an extensive mesh and solved by direct time domain approach, showed relatively large deviations as compared to those of the current and the sub structuring SSI methods. In the third example studied here, response spectrum analysis was provided using the proposed SSI approach which is based on the FE-IFE modeling and WT theory. The results were compared to conventional fixed based structural analysis. It was shown that SSI effects become significant when stiff structures rest on soils especially on soft mediums. Discussion on the results was also extended to the Iranian Building Code Requirements 2800 and comparisons were made.

## References

- ANSYS 5.4 (1997), *Basic analysis procedures guide*, 000856, 2<sup>nd</sup> Edition, SASIP, Inc.
- Bagheripour, M.H. and Marandi, S.M. (2003), "Analysis of static and dynamic problems in geotechnics with infinite elements", *Proceedings of Sixth International Conference in Civil Engineering, Isfahan University of Technology, Iran*.
- Bagheripour, M.H. and Marandi, S.M. (2005), "A numerical model for unbounded soil domain in earthquake SSI analysis using periodic infinite elements", *Int. J. Civil Eng.*, **3**(2), 96-111.
- Baziar Mansour Khani, M.H. (2007), "Dynamic soil-structure interaction analysis using the scaled boundary element method", *PhD thesis*, School of Civil and Environmental Engineering, The University of New South Wales, Sydney, Australia.
- Boore, D. (2008), "TSPP, A collection of FORTRAN programs for processing and manipulating time series", *U.S Geological Survey Open-File Report 2008-1111*, Version 1.2, March.
- Bettes, P. (1977), "Infinite elements", *Int. J. Numer. Meth. Eng.*, **11**, 355-375.
- Brinkgreve, R.B.J., Vermeer, P.A. and Bakker, K.J. (1988), *Material model manual*, PLAXIS V.7, A.A. Balkema, Rotterdam, Brookfield.
- Cattani, C. (2004), "Haar wavelet based on technique in evolution problems", *Proc. Estonian Academic Sci. Phys. Math.*, **51**, 45-63.
- Chen, C.F. and Hesiao, C.H. (1997), "Haar wavelet method for solving lumped and distributed-parameter systems", *IEE P. - Contr. Theor. Ap.*, **144**, 87-94.
- Chen, C.F. and Hesiao, C.H. (1997), "Wavelet approach to optimizing dynamic systems", *IEE P. - Contr. Theor. Ap.*, **144**, 213-219.
- Chore, H.S., Ingle, R.K. and Sawant, V.A. (2009), "Building frame-pile foundation-soil interactive analysis", *Interact. Multiscale Mech.*, **2**(4), 397-411.
- Chow, Y.K., and Smith, I.M. (1981), "Static and periodic infinite solid elements", *Int. J. Numer. Math. Eng.*, **17**, 503-526.
- Chuhan, Z. and Zhao, C. (1987), "Coupling method of finite and infinite elements for strip foundation wave problems", *Earthq. Eng. Struct. Dyn.*, **15**, 839-85.
- Cundall, P.A., Kunar, R.R., Carpenter, P.C. and Marti, J. (1978), "Solution of infinite dynamic problems by finite modeling in the time domain", *Conference on Applied Numerical Modelling*, Madrid.

- Darbre, G.R. and Wolf, J.P. (1988), "Criterion of stability and implementation issues of hybrid frequency-time domain procedure for non-linear dynamic analysis", *Earthq. Eng. Struct. Dyn.*, **16**, 569-581.
- Deneme, I.O., Yerli, H.R., Severcan, M.H., Tanrikulu, A.H. and Tanrikulu, A.K. (2009), "Use and comparison of different types of boundary elements for 2D soil-structure interaction problems", *Adv. Eng. Softw.*, **40**, 847-855.
- Ding, H.P. and Liao, Z.P. (2001), "A hybrid analysis method for linear dynamic soil-structure interaction in time and frequency domain", *ACTA Seismol. Sinica*, **14** (4), 440-447.
- Goedecker, S. and Ivanov, O. (1998), "Solution of multi scale partial differential equations using wavelets", *Comput. Phys.*, **12**(6), 548-555.
- Gouasmia, A. and Djeghaba, K. (2007), "Non-linear seismic soil-structure interaction analysis of structures based the substructure method", *Asian J. Civil Eng. (Bulid. Housing)*, **8**(2), 183-201.
- Heidari, A. (2004), "Optimum design of structures against earthquake by advanced optimization methods", *PhD thesis*, University of Kerman, Iran.
- Hsiao, C.H. and Wang, W.J. (2001), "Haar wavelet approach to nonlinear stiff systems", *Math. Comput. Simulat.*, **57**, 347-353.
- Kausel, E. (1974), "Forced vibration of circular foundations in layered media", *MIT Research Report R74-11*, MIT.
- Kausel, E. (2010), "Early history of soil-structure interaction", *J. Soil Dyn. Earthq. Eng.*, **30**, 822-832.
- Kim, D.K. (1999), "Analytical frequency-dependent infinite elements for soil-structure interaction analysis in time domain", *PhD Dissertation*, Korea Advanced Institute of Science and Technology, Korea.
- Kim, D.K. and Yun, C. (2000), "Time domain soil structure interaction analysis in two-dimensional medium based on analytical frequency dependant infinite elements", *Int. J. Numer. Meth. Eng.*, **47**, 1241-1261.
- Kramer, S. L. (1996), *Geotechnical earthquake engineering*, Prentice Hall, N.J.
- Lepik, U. (2004), "Numerical solution of differential equations using haar wavelets", *Math. Comput. Simulat.*
- Liao, Z.P., Wong, H.L. and Yifan, Y. (1984), "A transmitting boundary for transient wave analysis", *J. Eng. Mech. Division - ASCE*, **27**, 1063-1073.
- Logan, D. L. (2008), *A first course in the finite element method*, 4th Edition, Thompson.
- Lysmer, J. and Kuhlemeyer, R.L. (1969), "Finite dynamic model for infinite media", *J. Eng. Mech. Division - ASCE*, **95**, 850-877.
- Masia, M.J., Kleeman, P.W. and Melchers, R.E. (2004), "Modeling soil-structure interaction for masonry structures", *J. Struct. Eng. - ASCE*, **130**(4), 641-649.
- Matlab R2009B, Version 7.9.0.529, Mathworks Inc., USA.
- Nakhaei, M. and Ghannad, M.A. (2006), "The effect of soil-structure interaction on hysteretic energy demand of buildings", *Struct. Eng. Mech.*, **24**(5), 641-645.
- Riddell, R. and Garcia, J.E. (2001), "Hysteretic energy spectrum and damage control", *Earthq. Eng. Struct. Dyn.*, **30**, 1791-1816.
- Tabatabaiefar, H.R. and Massumi, A. (2010), "A simplified method to determine seismic responses of reinforced concrete moment resisting building frames under influence of soil-structure interaction", *J. Soil Dyn. Earthq. Eng.* (in press)
- Wang, J. (2005), "Influence of different boundary conditions on analysis of SSI", *Proceedings of 18<sup>th</sup> International Conference on Structural Mechanics in Reactor Technology (SMIRT 18)*, Beijing China, August 7-12.
- White, W., Valliappan, S. and Lee, I.K. (1977), "Unified boundary for finite dynamic models", *J. Eng. Mech. Division - ASCE*, **103**, 949-964.
- Wolf, J.P. (1985), *Dynamic soil structure interaction*, Prentice Hall, Englewood Cliffs, N.J.
- Wolf, J.P. (1994), *Foundation vibration analysis using simple physical models*, Prentice-Hall, Englewood Cliffs, NJ.
- Yun, C.B., Kim, D.K. and Kim, J.M. (2000), "Analytical frequency-dependent infinite elements for soil-structure interaction analysis in two dimensional medium", *Eng. Struct.*, **22**, 258-271.
- Zhao, C., Valliappan, S. and Wang, Y.C. (1991), "An approximate method for simulating infinite media", *Comput. Struct.*, **41**(5), 1041-1049.
- Zhao, C. and Valliappan, S.A. (1992), "Dynamic infinite element for 3-D infinite domain wave problems", *Int. J.*

*Numer. Math. Eng.*, **36**, 2567-2580.

Zhao, C. and Zhang, C. (1989), "Analysis of 3-D foundation wave problems by mapped dynamic infinite elements", *J. Sci. China*, **32**(4), 479-491.

CC